HHS Public Access

Author manuscript

J Biomed Nanotechnol. Author manuscript; available in PMC 2017 June 01.

Published in final edited form as:

J Biomed Nanotechnol. 2016 June ; 12(6): 1303–1311.

Polyanhydride Nanovaccines Induce Germinal Center B Cell Formation and Sustained Serum Antibody Responses

Julia E. Vela Ramirez[1], **Lorraine T. Tygrett**[2], **Jihua Hao**[3], **Habtom H. Habte**[4,5], **Michael W. Cho**[4,5], **Neil S. Greenspan**[3], **Thomas J. Waldschmidt**[2], and **Balaji Narasimhan**[1,*]

[1]Department of Chemical and Biological Engineering, Iowa State University, Ames, IA 50011, USA

[2]Department of Pathology, University of Iowa, Iowa City, IA 52242, USA

[3]Department of Pathology, Case Western Reserve University, Cleveland, OH 44106, USA

[4]Department of Biomedical Sciences, Iowa State University, Ames, IA 50011, USA

[5]Center for Advanced Host Defenses, Immunobiotics and Translational Comparative Medicine, Iowa State University, Ames, IA 50011, USA

Abstract

Biodegradable polymeric nanoparticle-based subunit vaccines have shown promising characteristics by enhancing antigen presentation and inducing protective immune responses when compared with soluble protein. Specifically, polyanhydride nanoparticle-based vaccines (i.e., nanovaccines) have been shown to successfully encapsulate and release antigens, activate B and T cells, and induce both antibody- and cell-mediated immunity towards a variety of immunogens. One of the characteristics of strong thymus-dependent antibody responses is the formation of germinal centers (GC) and the generation of GC B cells, which is part of the T helper cell driven cellular response. In order to further understand the role of nanovaccines in the induction of antigen-specific immune responses, their ability to induce germinal center B cell formation and isotype switching and the effects thereof on serum antibody responses were investigated in these studies. Polyanhydride nanovaccines based on 1,6-bis(*p*-carboxyphenoxy)hexane and 1,8-bis(*p*-carboxyphenoxy)-3,6-dioxaoctane were used to subcutaneously administer a viral antigen. GC B cell formation and serum antibody responses induced by the nanovaccines were compared to that induced by alum-based vaccine formulations. It was demonstrated that a single dose of polyanhydride nanovaccines resulted in the formation of robust GCs and serum antibody in comparison to that induced by the alum-based formulation. This was attributed to the sustained release of antigen provided by the nanovaccines. When administered in a multiple dose regimen, the highest post-immunization titer and GC B cell number was enhanced, and the immune response induced by the nanovaccines was further sustained. These studies provide foundational information on the mechanism of action of polyanhydride nanovaccines.

*Author to whom correspondence should be addressed. nbalaji@iastate.edu.

Keywords

Nanovaccine; Germinal Center; Polyanhydride; T Helper Cells; Antibody

INTRODUCTION

The design of novel adjuvant formulations to improve vaccine efficacy by inducing strong immune responses towards a variety of pathogens is one of the main goals in the development of new generation vaccines. In this regard, nanoparticle-based systems have shown desirable characteristics because they provide dual functions as adjuvants and delivery vehicles.[1–3] Among these systems, biodegradable polymers have been shown to stimulate the immune system and induce protective immunity.[3] In particular, polyanhydride nanoparticles have demonstrated the ability to stimulate and activate antigen presenting cells (APCs), induce both cellular and robust antibody responses with a variety of antigens, and provide protective immunity with a single dose.[4,5] Antigen transport and presentation by APCs to B cells and T cells in the draining lymph node is one of the first steps in the induction of potent immune responses.

Previous studies have shown the ability of biodegradable and non-degradable nanoparticles to induce antibody responses with multiple antigens.[6,7] In particular, the use of polymeric nanoparticle systems for drug and vaccine delivery offers several advantages, including controlled delivery of encapsulated payload(s), and depending on their chemistry, improved biocompatibility, receptor targeting capabilities, sustained antigen/drug release kinetics, adjuvanticity, and opportunities for both local and systemic delivery.[8,9] Among these systems, polyanhydride nanoparticles have displayed many of these characteristics in both *in vitro* and/or *in vivo* settings.[4, 10–17] The polyanhydride nanoparticle-based platform offers multiple advantages compared to other polymeric systems (i.e., poly(lactide-co-glycolide) nanoparticles or liposomes), because of their surface erosion mechanism that leads to predictable payload release kinetics, milder pH microenvironments, and the ability to stabilize fragile antigens.[10, 18–21]

Even though polyanhydride nanoparticle-based vaccines (i.e., nanovaccines) have been demonstrated to induce protective antibody-driven immune responses, their ability to induce germinal center (GC) B cells, and to hence activate the T helper cell driven cellular response, has not been investigated. Therefore, the main focus of these studies was the analysis of GC B cells and T follicular helper cells in the draining lymph nodes of animals immunized subcutaneously with vaccines based on two different adjuvants: alum and polyanhydride nanoparticles. The induction of serum antibodies to the immunizing antigen was also measured. In this work, an engineered derivative of an HIV-1 protein (gp41-54Q-GHC) was used as a model antigen. The results obtained showed that polyanhydride nanovaccines induced GC B cell formation and T follicular helper cells, which led to robust serum antibody responses. In addition, it was shown that multiple immunizations improved the performance of the polyanhydride nanovaccines with respect to generating more GC B cells and robust antibody responses.

MATERIALS AND METHODS

Materials

Chemicals needed for monomer synthesis, polymerization, and nanoparticle synthesis included anhydrous (99+%) 1-methyl-2-pyrrolidinone (Aldrich, Milwaukee, WI); 1,6-dibromohexane, 4-*p*-hydroxybenzoic acid, *N,N*-dimethylacetamide, triethylene glycol and Span® 80 (Sigma Aldrich, St. Louis, MO); 4-*p*-fluorobenzonitrile (Apollo Scientific, Cheshire, UK); acetic acid, acetic anhydride, acetone, acetonitrile, dimethyl formamide (DMF), hexanes, methylene chloride, pentane, potassium carbonate, sodium hydroxide, sulfuric acid, and toluene (Fisher Scientific, Fairlawn, NJ). For NMR characterization, deuterated dimethyl sulfoxide was purchased from Cambridge Isotope Laboratories (Andover, MA).

Construction, Expression and Purification of pET-gp41-54Q-GHC

The plasmid encoding gp41-54Q-GHC was constructed based on pET-gp41-54Q, which encodes 54 amino acids of the C-terminal ectodomain of HIV-1 gp41 (based on M group consensus sequence, MCON6). The terminal lysine residue was mutated to glutamine. A short linker (GSGSG), followed by a 6xHis tag and a cysteine residue (C), was attached right after the glutamine by PCR using a forward primer 5′-CGCGGATCCGAGTGGGAGCGC GAGATC-3′ and a reverse primer 5′-CCATGAATTCTT AGCAATGGTGATGATGGTGATGTCCCGATCCCGATC CCTGGATGTACCACAGCCAGTT-3′. The PCR product was digested by BamHI and EcoRI and then ligated into corresponding sites in pET-21a to yield pET-gp41-54Q-GHC. The construct was confirmed by sequencing. Protein expression and purification were performed according to the method of Penn-Nicholson et al.[22] with a few modifications as described previously.[15]

Monomer and Polymer Synthesis

Monomers of 1,6-bis(*p*-carboxyphenoxy) hexane (CPH) and 1,8-bis(*p*-carboxyphenoxy)-3,6-dioxaoctane (CPTEG) were synthesized as described previously.[11, 23] A 20:80 CPTEG:CPH copolymer was synthesized by melt polycondensation as previously described.[11] The chemical structure was characterized with ^{1}H NMR using a Varian VXR 300 MHz spectrometer (Varian Inc., Palo Alto, CA). The synthesized 20:80 CPTEG:CPH copolymer had a M_w of 8,000 Da, and the polydispersity index (PDI) of this copolymer was 1.5, which is consistent with previous work.[4, 11]

Nanoparticle Synthesis and Characterization

Polyanhydride nanoparticles based on the 20:80 CPTEG:CPH chemistry were synthesized using antisolvent nanoencapsulation as described previously.[24] Briefly, lyophilized gp41-54Q-GHC (2% w/w) and Span® 80 (1% v/v) and 20 mg/mL of 20:80 CPTEG:CPH polymer were dissolved in methylene chloride (at 4 °C). The polymer solution was sonicated at 40 Hz for 30 s using a probe sonicator (Ultra Sonic Processor VC 130PB, Sonics Vibra Cell, Newtown, CT) and rapidly poured into a pentane bath (at −40 °C) at a solvent to non-solvent ratio of 1:250. Particles were collected by filtration and dried under vacuum for 30

min. Morphological and size characterization of the nanoparticles was performed using scanning electron microscopy (SEM, FEI Quanta 250, Kyoto, Japan) and quasi-elastic light scattering (QELS, Zetasizer Nano, Malvern Instruments Ltd., Worchester, UK).

Antigen Release Kinetics

In vitro antigen release kinetics studies were performed using a micro bicinchoninic acid (BCA) assay. Samples of protein-loaded nanoparticles were suspended in 750 μL of phosphate buffered saline (0.1 M, pH 7.4) with 0.01% w/v sodium azide and incubated at 37 °C and 106 rcf. For each time point, samples were centrifuged at 10,000 rcf for 10 min, the supernatant was removed and aliquoted at 4 °C, and fresh buffer was added to each sample to maintain perfect sink conditions. Aliquots were analyzed using the micro-BCA assay at an absorbance of 562 nm. The experiment was carried out for 30 days, and the amount of released protein was normalized with total amount of protein encapsulated, as described previously.[10, 21] After 30 days, the remaining protein was extracted by adding 750 μL of 17 mM NaOH solution. Protein encapsulation efficiency was estimated using the micro-BCA assay.

Mice

Specific pathogen free female BALB/c mice were purchased from the National Cancer Institute (Frederick, MD) and housed in barrier rooms at the University of Iowa Animal Care Facility. All mice used in the experiments were at least eight weeks of age. Animal procedures were approved by the University of Iowa Institutional Animal Care and Use Committee in accordance with Association for Assessment and Accreditation of Laboratory Animal Care, International (AAALAC International), and PHS Animal Welfare mandates.

Mouse Treatments

Preparation of Antigens and Immunizations—Separate groups of mice were subcutaneously injected with gp41-loaded 20:80 CPTEG:CPH nanoparticles or gp41 precipitated with a 10% $AlK(SO_4)_2$ solution (Alum). Nanoparticles were resuspended in phosphate buffer saline by probe sonication (Sonicator Model CL-18, Fisher Scientific, Pittsburgh, PA). Mice were immunized subcutaneously in both rear footpads with 250 μg of antigenloaded nanoparticles (2% w/w gp41-54Q-GHC-loaded) in a 50 μL volume (500 μg total per mouse containing a total of 10 μg of antigen). Single immunization experiments involved one administration of particle/antigen formulation and serum samples and popliteal draining lymph nodes (dLNs) were collected at days 8, 12 and 18 post-immunization. Multiple immunization regimens included the administration of particle/antigen formulations at days 0, 7 and 14. Serum samples and popliteal dLNs were collected at day 21 post-immunization.

Flow Cytometry—Popliteal dLNs were harvested from immunized mice at designated time points. To obtain single cell suspensions, dLNs were minced with frosted slides and washed with balanced salt solution. The cell suspensions were subjected to Fico/Lite-LM (Atlanta Biologicals, Norcross, GA) density centrifugation to obtain viable mononuclear cells, and resuspended in staining buffer (balanced salt solution, 5% bovine calf serum, and 0.1% sodium azide). About 0.5–1.0 million cells were stained with combinations of

fluorochrome-conjugated antibodies to identify various cell subsets. Non-specific binding of conjugated antibodies was inhibited by blocking cells with 10 μL of rat serum (Pel Freez, Rogers, AR) and 10 μg of 2.4G2, an anti-Fcγ R monoclonal antibody. Rat anti-mouse monoclonal antibodies used were anti-IgM (b7-6), anti-B220 (6B2), anti-CD44 (9F3), anti-CD4 (PerCP/Cy5.5 conjugate, BioLegend, San Diego, CA), anti-CD150 (PE conjugate, BioLegend, San Diego, CA) and anti-CXCR5 (biotin conjugate, BD Pharmingen, San Diego, CA). Goat anti-mouse antibodies used were biotin-labeled anti-IgG1, -IgG2a, -IgG2b, and -IgG3 (all from Southern Biotechnology Associates, Birmingham, AL). FITC-conjugated peanut agglutinin (PNA) was purchased from Vector Laboratories (Burlingame, CA). 2.4G2, b7-6, 6B2, 9F3 and 7D4 were semi-purified from HB101 serum-free supernatants using 50% ammonium sulfate precipitation. b7-6 was conjugated to biotin (Sigma-Aldrich, St. Louis, MO) and 6B2 and 9F3 were conjugated to Cy5 (Amersham Pharmacia, Piscataway, NJ) using standard procedures. Purified rat IgG (Jackson Immunoresearch Laboratories, West Grove, PA) was conjugated and used for isotype controls. Primary monoclonal antibodies or PNA were added to cells and incubated for 20 min on ice. For anti-CXCR5 staining, the primary incubation was 30 min at room temperature. After washing cells twice in staining buffer, PE-conjugated streptavidin (Southern Biotechnology Associates) was used to detect most biotinylated Abs. PE-Cy7-conjugated streptavidin (eBioscience, San Diego, CA) was used to detect biotin-conjugated anti-CXCR5 monoclonal antibody. Cells were incubated on ice for 20 min and resuspended in fixative (1% formaldehyde in 1.25X PBS) after washing twice with staining buffer. Stained cells were run on a FACSCanto II (Becton Dickinson, San Jose, CA). All data were analyzed using FlowJo software (Tree Star, Ashland, OR).

gp41-54Q-Specific Enzyme-Linked Immunosorbent Assay (ELISA)—Briefly, gp41-54Q-GHC (at 33 ng/well) was coated onto 96-well Nunc-Immuno Plates (Nunc; Cat # 439454) using antigen coating buffer (15 mM Na_2CO_3, 35 mM $NaHCO_3$, 3 mM NaN_3, pH 9.6) at 4 °C overnight. Non-specific antibody binding was prevented by blocking wells with PBS (pH 7.5) containing 2.5% skim milk and 25% FBS at 37 °C for one hour and the plates were washed four times with 0.1% Tween 20 in PBS. NP-40 was added to plasma samples (0.1% final) before dilution in blocking buffer. Antibodies and plasma samples were diluted as indicated, added to wells and incubated for two hours at 37 °C in 200 μL blocking buffer. Wells were washed four times, and secondary antibody goat anti-mouse IgG conjugated to horseradish peroxidase (Pierce; Cat # 31410) was incubated at 1:3,000 dilution at 37 °C for one hour. Wells were washed four times, and developed by adding 100 μL of TMB HRP-substrate (Bio-Rad) for 5–10 min. Reactions were stopped with 50 μL of 2 N H_2SO_4. Plates were read on a microplate reader (Versamax by Molecular Devices) at 450 nm. Experiments were performed in duplicate.

Statistical Analysis—Statistical significance was determined by two-way analysis of variance (ANOVA) followed by Tukey's post-test using GraphPad Prism software (Version 6.0, GraphPad Prism Software, Inc., La Jolla, CA).

RESULTS

Synthesis and Characterization of gp41-Loaded Polyanhydride Nanoparticles

Previous work has shown that amphiphilic nanoparticle chemistries exhibited desirable characteristics in terms of protein stabilization, robust antibody responses, activation of APCs, and induction of $CD8^+$ T cell responses.[4, 10, 12, 16, 25, 26] Specifically, it was demonstrated that 20:80 CPTEG:CPH nanoparticle formulations provided sustained release of stable gp41-54Q-GHC, as evidenced by the ability of the released antigen to be recognized by several HIV-1 monoclonal antibodies.[15] Based on these studies, the 20:80 CPTEG:CPH nanoparticle formulation was selected to carry out the studies described herein. Particle morphology was characterized using scanning electron microscopy as shown in Figure 1(panel A) and the size of these particles was measured using ImageJ software (version 1.47 v, NIH, Bethesda, MD). The size of the 20:80 CPTEG:CPH nanoparticles was 192±79 nm, which is consistent with previous studies.[13, 16, 18, 19, 24] The encapsulation efficiency of the antigen was ~90%, and as shown in Figure 1(panel B), the gp41-54Q-GHC-loaded nanoparticles displayed sustained antigen release kinetics over 21 days releasing ~80% of the encapsulated antigen, with an initial burst of ~45% of the encapsulated gp41-54Q-GHC within the first hour.

Single Immunization with Alum and Polyanhydride Nanovaccine Elicited Measurable Anti-gp41 Antibody

Following a single subcutaneous administration in the footpad of 10 μg of gp41-antigen to mice using the two aforementioned vaccine formulations, serum and dLNs were collected at 8, 12 and 18 days. As shown in Figure 2, serum antibody levels in animals treated with the gp41-antigen precipitated in alum formulation displayed higher titers at day 8 post-immunization than at days 12 or 18, reaching a maximum titer of 0.5×10^4 and waning to background levels by day 18. These results indicate that even though the alum-based formulation was able to induce a measurable immune response towards the gp41 antigen, the response induced was not robust or sustained. Therefore, we analyzed the quality of the immunity that was induced by this combination of antigen and adjuvant by measuring the amounts of GC B cells and T follicular helper cells in the popliteal lymph nodes using the gating strategy shown in Figure 3(panels A and B, respectively). The results shown in Figure 3(panel C) demonstrate that the numbers of GC B cells followed a bell shaped curve, with 5×10^4 cells present initially in the dLNs, followed by a peak, among time points sampled, at day 12 (consistent with the antibody secretion data) with 8×10^4 cells and returning to 4×10^4 cells by day 18. Similar trends were found in the numbers of T follicular helper cells as shown in Figure 3(panel D), but these numbers ranged from 0.5×10^4 to 1.5×10^4 cells over the course of the study.

Similar experiments were carried out using the gp41-54Q-GHC-loaded 20:80 CPTEG:CPH nanovaccine formulation. As shown in Figure 4, the serum antibody levels obtained with this vaccine formulation were more robust, reaching a titer of 2×10^4 within eight days post-vaccination, which was maintained through 18 days post-immunization (which was the duration of the study). To be able to directly compare the responses induced by the two different vaccine formulations used, quantification of the numbers of GC B cells and T

follicular helper cells in the dLNs was performed. Challenge with the nanovaccine resulted in a similar pattern of GC B cell and T follicular helper numbers in the dLNs compared with the alum formulation, although the total numbers were slightly lower as shown in Figure 5. Specifically, the highest number of GC B cells was observed at day 12 post-challenge and numbers of T follicular helper cells were higher early in the response and waned by day 18. However, the sustained release provided by the polyanhydride nanovaccine formulations more effectively enabled the maintenance of antibody titers after challenge with a single dose.

In order to analyze the quality of the GC B cell response elicited by the nanovaccine formulation, surface immunoglobulin isotype expression was determined on B cells from dLNs using the gating strategy shown in Figure 6(panel A). As shown in Figure 6(panel B), the majority of GC B cells (>60%) had switched to IgG (either IgG1, IgG2a/b, or IgG3) by day 12 post-challenge. Within the IgG switched GC B cell compartment, all subclasses were represented, with the majority expressing IgG1. This is expected for BALB/c mice given their propensity towards Th2 responses.

Multiple Immunization Regimen Using Polyanhydride Nanovaccine Elicited Robust Anti-gp41 Antibody Responses

In order to investigate if multiple immunizations with the polyanhydride nanovaccine induced even more robust immune responses, animals were immunized subcutaneously three times with gp41 antigen-loaded 20:80 CPTEG:CPH nanoparticles at 0, 7 and 14 days. As expected, the multiple immunization schedule resulted in the induction of a robust antibody response, with the titers reaching 10^5 by 21 days post the first dose as shown in Figure 7. In addition, 6×10^4 germinal center B cells were detected in the dLN 21 days post-immunization, which is higher than the number of cells detected at days 12 or 18 with a single immunization (Fig. 5). However, similar numbers (0.2×10^4) of T follicular helper cells were detected in the dLN at day 21 when compared to the number of T follicular helper cells at day 18, but lower than the day 8 numbers in the single immunization experiments.

Finally, the surface immunoglobulin isotype of GC B cells was assessed a week after the third immunization (day 21) using flow cytometry and the gating strategy described previously in Figure 6(panel A). Figure 8 shows that a multiple challenge regimen with the polyanhydride nanovaccine induced a response similar to the single immunization protocol in that the majority (>60%) of GC B cells switched to one of the IgG subclasses. Once again, IgG1 was the dominant subclass with IgG2a, IgG2b and IgG3 represented at lower percentages.

DISCUSSION

In this work we report on the ability of a polyanhydride nanovaccine to induce GC B cell and T follicular helper cell responses against a viral antigen following subcutaneous administration to mice.[27] A variety of adjuvants have been shown to elicit potent immune responses towards various antigens.[28] In order to rationally design formulations that can elicit robust and protective immune responses, it is necessary to understand the mechanisms by which these materials induce immune responses. In this regard, the ability to induce GC

B cells and serum antibody responses provides foundational information about the adjuvanticity of polyanhydride nanovaccines and this work describes a systematic study of the adjuvant properties of a polyanhydride nanovaccine delivery platform using a model viral antigen.

It is known that B cell responses that include GC formation and generation of long-lived plasma cells and memory B cells are dependent on $CD4^+$ T helper cells.[29] In the past several years, T follicular helper cells have been identified as the key $CD4^+$ T cell subset necessary to drive GC reactions and their long-lived products.[27] Moreover, recent work suggests that the limiting factor in GC B cell responses is access to help from T follicular helper cells.[30] The generation of long-lived plasma cells and memory B cells is a highly desirable outcome upon vaccination. The induction of long-lived plasma and memory B cells contributes significantly to immunological recall responses, which is important upon exposure (or re-exposure) to pathogens. The work presented herein showed that single immunization with alum formulations was only able to elicit poor and short-lived antibody responses towards the gp41 antigen as shown in Figure 2. These observations suggest that the generated plasma cells were short lived. In contrast, immunizing with the polyanhydride nanovaccine induced moderate antibody responses, which were sustained for up to 18 days post-immunization as shown in Figure 4 due to prolonged antigen exposure enabled by the polyanhydride nanovaccine. In addition, both vaccine formulations induced the formation of GC B cells and T follicular helper cells, with the responses peaking at 12 days post-immunization, consistent with their antibody responses.

The relationship between GC formation and robust immune responses is influenced by the length of antigen exposure.[27] It has been shown previously that T follicular helper cell activation and differentiation is a multi-step process that requires antigen presentation by dendritic cells (DCs) in the T cell zone at early phases, and by activated B cells at the T cell-B cell border or in the follicle at later phases.[27] As such, the prolonged release of encapsulated antigen that occurs upon degradation of the nanoparticles (as shown in Fig. 1) should serve to activate T follicular helper cells much better than a single bolus of alum precipitated antigen.[12, 31–33] The data obtained in our experiments indicate that the sustained antigen release enabled by the polyanhydride nanoparticles may be critical for the induction of robust immune responses. This observation is consistent with other studies from our laboratories that also demonstrate the importance of sustained antigen release kinetics in the maintenance of long-lived antibody with high avidity.[4, 25, 34]

As stated above, the role of antigen presenting DCs is critical during the early phases of T follicular helper cell differentiation.[27] In previous studies, polyanhydride nanoparticles have demonstrated the ability to activate APCs[13, 26] and induce phenotypes that migrate to the lymph nodes. Based on the induction of T follicular helper cells by the vaccine formulations studied herein (as shown in Figs. 3, 5, and 7), it can be hypothesized that all of these formulations successfully activated DCs. Further improvements in the activation of DCs by polyanhydride nanoparticles could be achieved by the use of mechanisms targeting DCs as suggested in several studies.[13, 35, 36]

T follicular helper cells are known to play an important role in the induction of isotype switching and somatic hypermutation in GC B cells, as well as the formation of plasma and memory B cells.[29, 30, 37] T follicular helper cells promote GC responses by providing key survival and differentiation signals through both cell bound and soluble factors.[29] An important consideration in the development of vaccines is the quality of the antibody response elicited by the formulation, which is characterized by the isotype profile and the avidity of the antibody.[38] It is therefore noteworthy that the majority of GC B cells induced by the polyanhydride nanovaccine were isotype switched, and included all of the downstream IgG subclasses (Figs. 6 and 8). Antibody responses involving multiple switched immunoglobulin isotypes, especially when induced with mild inflammatory stimuli,[31] are important to neutralize viral pathogens that attack tissues such as the lungs where it is important to not induce overt inflammation.

In previous work, a single intranasal administration of polyanhydride nanovaccines demonstrated the ability to induce high titer antibody and confer protective immunity upon lethal challenge with bacterial pathogens.[4, 17, 39] The current work builds upon these studies by evaluating the mechanisms by which these novel biodegradable nanovaccine formulations induce strong antibody responses. Overall, the successful induction of long-lived antibody against viral pathogens, the expansion of T follicular helper cells and the generation of GC B cells are important components of mounting robust and effective immune responses specific for pathogen-derived antigens. The polyanhydride nanovaccine platform has been demonstrated to exhibit all of these components, making it a promising vehicle for vaccine development.

CONCLUSIONS

The studies reported herein demonstrate the ability of a polyanhydride nanovaccine to induce long-lived antibody against viral pathogens, expand T follicular helper cells and stimulate GC formation, especially in comparison to alum-based vaccines. Low antibody titers were obtained from subcutaneous immunization of mice from alum-based vaccine formulations. In contrast, more potent antibody responses involving isotype switching were induced by the polyanhydride nanovaccines. Together, these studies demonstrate the ability of the polyanhydride nanovaccine platform to elicit robust antibody-mediated immune responses *in vivo* and provide foundational information to evaluate the capabilities of this novel platform for vaccine delivery.

Acknowledgments

The authors would like to acknowledge financial support from NIH-NIAID (U19 AI-091031). MWC has an equity interest in NeoVaxSyn Inc., and serves as CEO/President. NeoVaxSyn Inc. did not contribute to this work or the interpretation of the data.

References

1. Kumari A, Yadav SK, Yadav SC. Biodegradable polymeric nanoparticles based drug delivery systems. Coll Surf B. 2010; 75:1.
2. De Jong WH, Borm PJ. Drug delivery and nanoparticles: Applications and hazards. Int J Nanomed. 2008; 3:133.

3. Sahdev P, Sahdev L, Ochyl J. Biomaterials for nanoparticle vaccine delivery systems. Pharm Res. 2014; 31:2563. [PubMed: 24848341]
4. Ulery BD, Kumar D, Ramer-Tait AE, Metzger DW, Wannemuehler MJ, Narasimhan B. Design of a protective single-dose intranasal nanoparticle-based vaccine platform for respiratory infectious diseases. PLoS One. 2011; 6:e17642. [PubMed: 21408610]
5. Huntimer L, Welder JHW, Ross KA, Carrillo-Conde B, Pruisner L, Wang C, Narasimhan B, Wannemuehler MJ, Ramer-Tait AE. Single immunization with a suboptimal antigen dose encapsulated into polyanhydride microparticles promotes high titer and avid antibody responses. J Biomed Mater Res B. 2013; 101:91.
6. Gregory AE, Titball R, Williamson D. Vaccine delivery using nanoparticles. Front Cell Infec Microbiol. 2013; 3:13. [PubMed: 23532930]
7. Zhao L, Seth A, Wibowo N, Zhao CX, Mitter N, Yu C, Middleberg APJ. Nanoparticle vaccines. Vaccine. 2014; 32:327. [PubMed: 24295808]
8. Mansour HM, Rhee YS, Wu X. Nanomedicine in pulmonary delivery. Int J Nanomed. 2009; 4:299.
9. Nguyen J, Steele TW, Merkel O, Reul R, Kissel T. Fast degrading polyesters as siRNA nano-carriers for pulmonary gene therapy. J Contr Rel. 2008; 132:243.
10. Torres MP, Determan AS, Anderson GL, Mallapragada SK, Narasimhan B. Amphiphilic polyanhydrides for protein stabilization and release. Biomaterials. 2007; 28:108. [PubMed: 16965812]
11. Torres MP, Vogel BM, Narasimhan B, Mallapragada SK. Synthesis and characterization of novel polyanhydrides with tailored erosion mechanisms. J Biomed Mater Res A. 2006; 76:102. [PubMed: 16138330]
12. Carrillo-Conde B, Schiltz E, Yu J, Minion FC, Phillips GJ, Wannemuehler MJ, Narasimhan B. Encapsulation into amphiphilic polyanhydride microparticles stabilizes Yersinia pestis antigens. Acta Biomater. 2010; 6:3110. [PubMed: 20123135]
13. Carrillo-Conde B, Song EH, Chavez-Santoscoy AV, Phanse Y, Ramer-Tait AE, Pohl NL, Wannemuehler MJ, Bellaire BH, Narasimhan B. Mannose-functionalized “pathogen-like” polyanhydride nanoparticles target C-type lectin receptors on dendritic cells. Mol Pharm. 2011; 8:1877. [PubMed: 21882825]
14. Chavez-Santoscoy AV, Roychoudhury R, Pohl NL, Wannemuehler MJ, Narasimhan B, Ramer-Tait AE. Tailoring the immune response by targeting C-type lectin receptors on alveolar macrophages using “pathogen-like” amphiphilic polyanhydride nanoparticles. Biomaterials. 2012; 33:4762. [PubMed: 22465338]
15. Ramirez JEV, Roychoudhury R, Habte HH, Cho MW, Pohl NL, Narasimhan B. Carbohydrate-functionalized nanovaccines preserve HIV-1 antigen stability and activate antigen presenting cells. J Biomat Sci Polym Ed. 2014; 25:1387.
16. Huntimer LM, Ross KA, Darling RJ, Winterwood NE, Boggiatto PM, Narasimhan B, Ramer-Tait AE, Wannemuehler MJ. Polyanhydride nanovaccine platform enhances antigen-specific cytotoxic T cell responses. Technology. 2014; 2:171.
17. Ross KA, Haughney SL, Petersen LK, Boggiatto PM, Wannemuehler MJ, Narasimhan B. Lung deposition and cellular uptake behavior of pathogen-mimicking nanovaccines in the first 48 hours. Adv Health Mater. 2014; 3:1071.
18. Haughney SL, Petersen LK, Ramer-Tait AE, King J, Schoofs A, Briles D, Wannemuehler MJ, Narasimhan B. Retention of structure, antigenicity, and biological function of pneumococcal surface protein A (PspA) released from polyanhydride nanoparticles. Acta Biomater. 2013; 9:8262. [PubMed: 23774257]
19. Petersen LK, Phanse Y, Ramer-Tait AE, Wannemuehler MJ, Narasimhan B. Amphiphilic polyanhydride nanoparticles stabilize Bacillus anthracis protective antigen. Mol Pharm. 2012; 9:874. [PubMed: 22380593]
20. Ross KA, Wu W, Loyd H, Huntimer L, Wannemuehler MJ, Carpenter S, Narasimhan B. Structural and antigenic stability of H5N1 hemagglutinin trimer upon release from polyanhydride nanoparticles. J Biomed Mater Res A. 2014; 102:4161. [PubMed: 24443139]

21. Lopac SK, Torres MP, Wilson-Welder JH, Wannemuehler MJ, Narasimhan B. Effect of polymer chemistry and fabrication method on protein release and stability from polyanhydride microspheres. J Biomed Mater Res B. 2009; 91:938.
22. Penn-Nicholson A, Han DP, Kim SJ, Park H, Ansari R, Montefiori DC, Cho MW. Assessment of antibody responses against gp41 in HIV-1-infected patients using soluble gp41 fusion proteins and peptides derived from M group consensus envelope. Virology. 2008; 372:442. [PubMed: 18068750]
23. Conix A. Poly[1,3-bis(p-carbxoyphenoxy)-propane anhydride]. Macro Synth. 1966; 2:95.
24. Ulery BD, Phanse Y, Sinha A, Wannemuehler MJ, Narasimhan B, Bellaire BH. Polymer chemistry influences monocytic uptake of polyanhydride nanospheres. Pharm Res. 2009; 26:683. [PubMed: 18987960]
25. Haughney SL, Ross KA, Boggiatto PM, Wannemuehler MJ, Narasimhan B. Effect of nanovaccine chemistry on humoral immune response kinetics and maturation. Nanoscale. 2014; 6:13770. [PubMed: 25285425]
26. Torres MP, Wilson-Welder JH, Lopac SK, Phanse Y, Carrillo-Conde B, Ramer-Tait AE, Bellaire BH, Wannemuehler MJ, Narasimhan B. Polyanhydride microparticles enhance dendritic cell antigen presentation and activation. Acta Biomater. 2011; 7:2857. [PubMed: 21439412]
27. Crotty S. T follicular helper cell differentiation, function, and roles in disease. Immunity. 2014; 41:529. [PubMed: 25367570]
28. Vogel FR. Improving vaccine performance with adjuvants. Clin Infect Dis. 2000; 30:S266–70. [PubMed: 10875797]
29. Kim Y, Zliu, Tanaka S, Tran DQ, Chung Y. Regulation of germinal center reactions by B and T cells. Antibodies. 2013; 2:554.
30. Gitlin AD, Shulman Z, Nussenzweig MC. Clonal selection in the germinal centre by regulated proliferation and hypermutation. Nature. 2014; 509:637. [PubMed: 24805232]
31. Hutchison S, Benson RA, Gibson VB, Pollock AH, Garside P, Brewer JM. Antigen depot is not required for alum adjuvanticity. FASEB J. 2012; 26:1272. [PubMed: 22106367]
32. Chen YC, Hung WH, Lin G. Assessment of gold nanoparticles as a size-dependent vaccine carrier for enhancing the antibody response against synthetic foot-and-mouth disease virus peptide. Nanotechnology. 2010; 21:195101. [PubMed: 20400818]
33. Kipper MJ, Shen EE, Determan AS, Narasimhan B. Design of an injectable system based on bioerodible polyanhydride microspheres for sustained drug delivery. Biomaterials. 2002; 23:4405. [PubMed: 12219831]
34. Kipper MJ, Wilson JH, Wannemuehler MJ, Narasimhan B. Single dose vaccine based on biodegradable polyanhydride microspheres can modulate immune response mechanism. J Biomed Mater Res A. 2006; 76:798. [PubMed: 16345084]
35. Phanse Y, Carrillo-Conde BR, Ramer-Tait AE, Roychoudhury R, Pohl NLB, Wannemuehler MJ, Narasimhan B, Bellaire BH. Functionalization of polyanhydride microparticles with di-mannose influences uptake by and intracellular fate within dendritic cells. Acta Biomater. 2013; 9:8902. [PubMed: 23796408]
36. Goodman JT, Ramirez JEV, Roychoudhury R, Boggiatto PM, Pohl NLB, Wannemuehler MJ, Narasimhan B. Nanoparticle chemistry and functionalization differentially regulates dendritic cell —nanoparticle interactions and triggers dendritic cell maturation. Part Part Syst Charac. 2014; 31:1269.
37. Shulman Z, Gitlin AD, Weinstein JS, Lainez B, Esplugues E, Flavell RA, Craft JE, Nussenzweig MC. Dynamic signaling by T follicular helper cells during germinal center B cell selection. Science. 2014; 345:1058. [PubMed: 25170154]
38. Wilson-Welder JH, Torres MP, Kipper MJ, Mallapragada SK, Wannemuehler MJ, Narasimhan B. Vaccine adjuvants: Current challenges and future approaches. J Pharm Res. 2009; 98:1278.
39. Ulery BD, Petersen LK, Phanse Y, Kong CS, Broderick SR, Kumar D, Ramer-Tait AE, Carrillo-Conde B, Bellaire BH, Rajan K, Wannemuehler MJ, Metzger DW, Narasimhan B. Rational design of pathogen-mimicking amphiphilic materials as nanoadjuvants. Sci Rep. 2011; 1:198. [PubMed: 22355713]

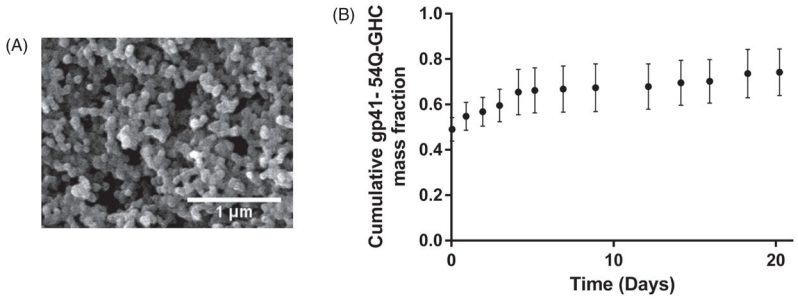

Figure 1.

gp41-54Q-GHC antigen release kinetics from polyanhydride nanoparticles and structural characterization from scanning electron photomicrographs. Panel A shows a scanning electron photomicrograph of gp41-54Q-GHC-loaded 20:80 CPTEG:CPH nanoparticles. Scale bar: 1 μm. Panel B shows the cumulative fraction of gp41-54Q-GHC released (•) from the 20:80 CPTEG:CPH nanoparticles. Error bars represent standard error of the mean; results are representative of three independent experiments.

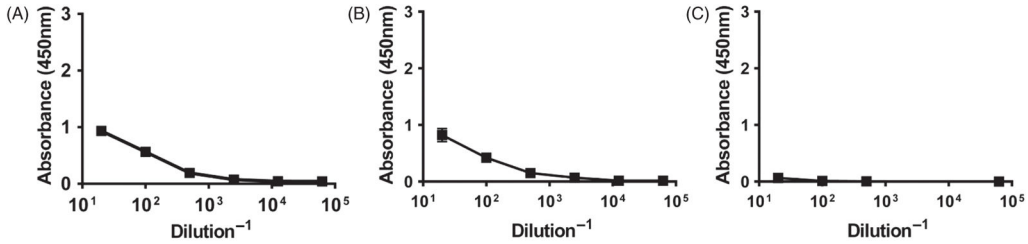

Figure 2.

Serum antibody response induced by single immunization with Alum formulation. BALB/c mice were injected s.c. with gp41-protein precipitated in alum. Serum samples were collected at days 8 (Panel A), 12 (Panel B) and 18 (Panel C) post-challenge and antibody titers were measured via ELISA. Plates were scanned at 450 nm.

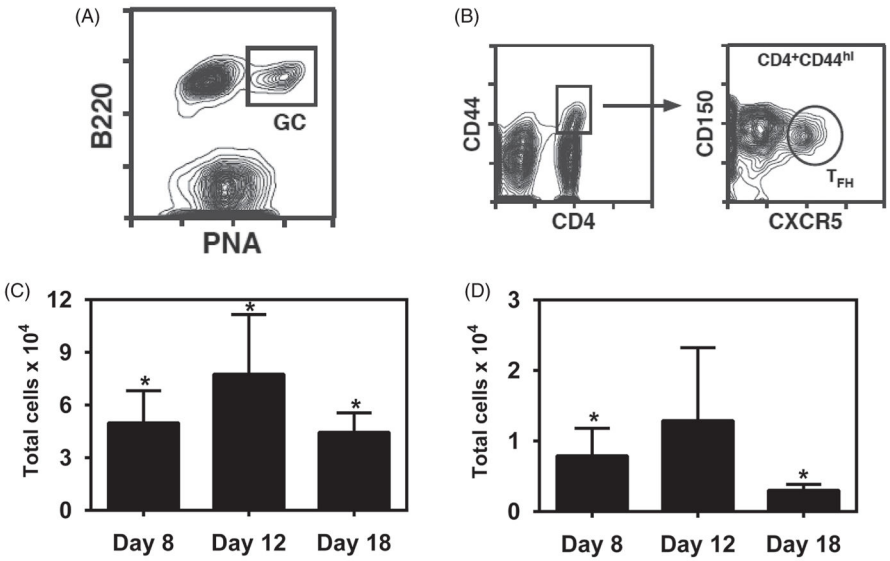

Figure 3.

B cell and T cell responses induced by single immunization with Alum formulation. BALB/c mice were injected s.c. with 10 μg of gp41-54Q-GHC precipitated in Alum. dLNs were harvested at days 8, 12 and 18 post-challenge and cell suspensions stained with either PNA and anti-B220 mAb, or with anti-CD4, anti-CD44, anti-CXCR5 and anti-CD150 mAbs. Stained cells were analyzed by flow cytometry. Panel A shows the gating strategy used in flow cytometric analysis of $B220^{hi}PNA^{hi}$ germinal center B cells from lymph nodes of BALB/c mice. Panel B shows the gating strategy used for selecting $CD4^{+}CD44^{hi}CXCR5^{+}CD150^{lo}$ T follicular helper cells. GC B cell bar graphs (Panel C) represent the total number of $B220^{+}PNA^{hi}$ GC B cells per LN from mice at each time point. T_{FH} bar graphs (Panel D) represent the total number of $CD4^{+}CD44^{hi}CXCR5^{+}CD150^{lo}$ T_{FH} cells per LN at each time point. Each bar represents mean±SEM. $n = 4–6$ mice at each time point. *Represents statistically significant differences between sample groups and background signal ($p < 0.05$).

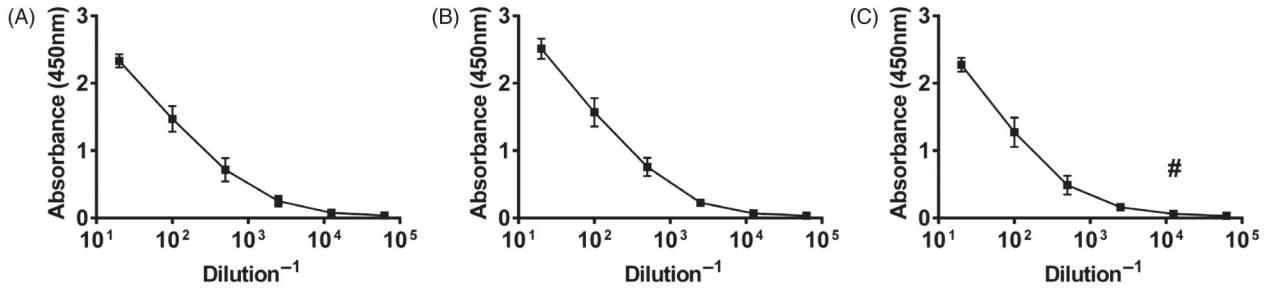

Figure 4.

Serum antibody response induced by single immunization with 20:80 CPTEG:CPH nanovaccine. BALB/c mice were injected s.c. with 500 μg total of gp41-loaded 20:80 CPTEG:CPH nanovaccine. Serum samples were collected at days 8 (Panel A), 12 (Panel B) and 18 (Panel C) post-challenge and antibody titers were measured via ELISA. Plates were scanned at 450 nm. #Represents statistically significant differences compared to Alum-treated groups at the same time point (p <0.05).

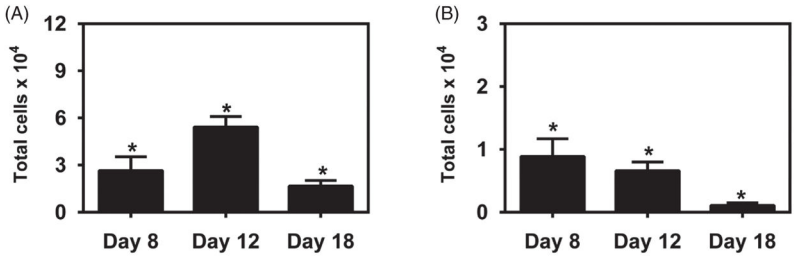

Figure 5.

B cell and T cell responses induced by single immunization with polyanhydride nanovaccine. BALB/c mice were injected s.c. with 500 μg total of gp41-loaded 20:80 CPTEG:CPH nanovaccine. dLNs were harvested at days 8, 12 and 18 post-challenge and cell suspensions stained with either PNA and anti-B220 mAb, or with anti-CD4, anti-CD44, anti-CXCR5 and anti-CD150 mAbs. Stained cells were analyzed by flow cytometry. GC B cell bar graphs (Panel A) represent the total number of $B220^{+}PNA^{hi}$ GC B cells per LN from mice at each time point. T_{FH} bar graphs (Panel B) represent the total number of $CD4^{+}CD44^{hi}CXCR5^{+}CD150^{lo}$ T_{FH} cells per LN at each time point. Each bar represents mean±SEM. n = 4–6 mice at each time point. *Represents statistically significant differences between sample groups and background signal (p <0.05).

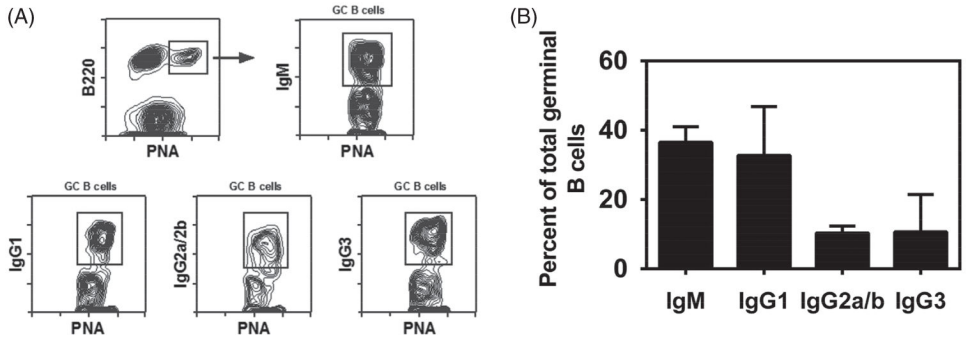

Figure 6.

Isotype distribution of GC B cells after single immunization with polyanhydride nanovaccine. BALB/c mice were injected s.c. with 500 μg total of gp41-loaded 20:80 CPTEG:CPH nanovaccine. dLNs were harvested 12 days after the challenge. Cell suspensions were stained with PNA, anti-B220 mAb, anti-IgM mAb and either goat anti-IgG1, IgG2a+IgG2b (BALB/c), or IgG3 specific Abs. Stained cells were analyzed by flow cytometry. Panel A shows the gating strategy used in flow cytometry for identification of IgM^+, $IgG1^+$, $IgG2a^+$/$IgG2b^+$, and $IgG3^+$ germinal center B cells from lymph nodes of BALB/c mice. IgM^+, $IgG1^+$, $IgG2^+$ and $IgG3^+$ B cells are shown as a percent of total GC B cells in Panel B. Each bar represents mean±SEM. n =4 mice at each time point.

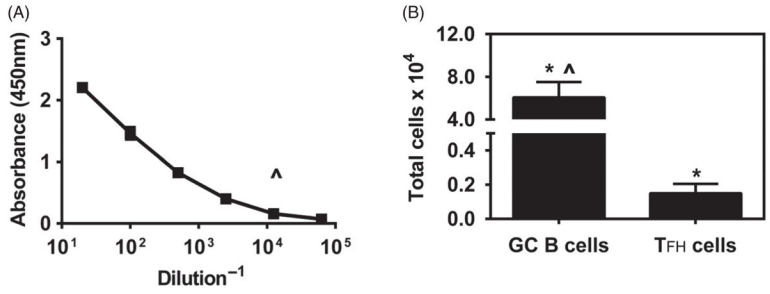

Figure 7.

Serum antibody and B cell and T cell responses to multiple immunizations with polyanhydride nanovaccine. BALB/c mice were injected s.c. with 500 μg of antigen loaded 20:80 CPTEG:CPH nanoparticles on days 0, 7 and 14. Serum samples were collected at day 21 post-challenge and antibody titers (Panel A) were measured via ELISA. Plates were scanned at 450 nm. dLNs were harvested 7 days after the last challenge (day 21). Total numbers of GC B cells and T_{FH} cells per LN (Panel B) were determined as described in the legend to Figure 3. Each bar represents mean±SEM. n = 4 mice at each time point. ^Represents statistically significant differences compared to Alum-treated groups at day 18. *Represents statistically significant differences between sample groups and background signal (p <0.05).

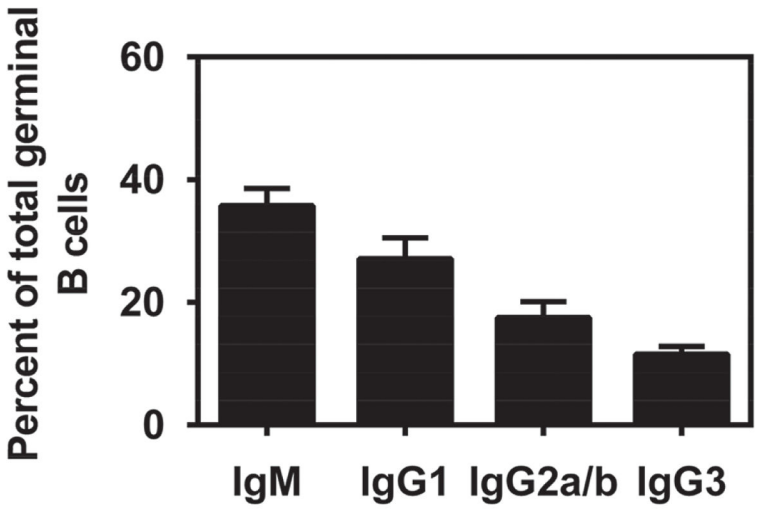

Figure 8.

Isotype distribution of GC B cells after multiple immunizations with polyanhydride nanovaccine. BALB/c mice were injected s.c. with 500 μg of antigen loaded 20:80 CPTEG:CPH nanoparticles on days 0, 7 and 14. dLNs were harvested 7 days after the last challenge (day 21). The proportion of IgM^+, $IgG1^+$, $IgG2a^+$/$IgG2b^+$, and $IgG3^+$ B cells within the $B220^{hi}PNA^{hi}$ GC B cell compartment was determined as described in the legend to Figure 6. Each bar represents mean±SEM. n = 4 mice at each time point.